THE JOURNAL OF PROSTHETIC DENTISTRY

RESEARCH AND EDUCATION

Effect of different laser modalities and treatment methods on the surface roughness and alterations of 3D printed resins and PEEK: An in vitro study

Irem Celikyurek Karabagli, DDS, PhD,[a] Akanay Copuroglu, DDS, PhD,[b] Zeynep Ozkurt-Kayahan, DDS, PhD,[c] and Ozgun Yusuf Ozyilmaz, DDS, PhD[d]

ABSTRACT

Statement of problem. The effects of laser irradiation, airborne-particle abrasion, and electrolytic cleaning on the surface roughness of 3-dimensionally (3D) printed resin and PEEK healing abutments remain unclear.

Purpose. The purpose of this in vitro study was to examine surface changes after different treatment methods were applied to the surfaces of the different 3D printed resin and PEEK materials used as custom healing abutments.

Material and methods. Disk-shaped specimens (3×10 mm) were fabricated from three 3D printed resins (VarseoSmile TriniQ, Saremco Print Crowntec, C&B Ceramic Resin) and PEEK (CopraPeek) (N=240). Specimens were assigned to 5 surface treatment groups: erbium-doped yttrium aluminum garnet (Er:YAG), neodymium-doped yttrium aluminum garnet (Nd:YAG), diode laser, airborne-particle abrasion, and GalvoSurge (n=48). Surface roughness (Ra) was measured at baseline (T0) and after treatment (T1). Representative specimens were examined using scanning electron microscopy (SEM). Data were analyzed using nonparametric tests (α=.05).

Results. Airborne-particle abrasion and Er:YAG significantly increased surface roughness in all groups (P<.05). The highest roughness was observed in the Crowntec–airborne-particle abrasion group (0.89 ±0.09 µm), and the lowest in the TriniQ–GalvoSurge group (0.09 ±0.02 µm). GalvoSurge caused no significant change in TriniQ and PEEK but increased roughness in C&B and Crowntec. Nd:YAG showed no effect in TriniQ and C&B but increased roughness in Crowntec and PEEK, while diode laser affected only Crowntec (P<.05). SEM analysis confirmed treatment-dependent surface morphology changes.

Conclusions. Surface treatments altered resin and PEEK surface properties. Airborne-particle abrasion and Er:YAG laser treatments resulted in the greatest increases in surface roughness, while GalvoSurge and diode laser treatments generally caused minimal or nonsignificant changes. (J Prosthet Dent xxxx;xxx:xxx-xxx)

The success of implant-supported prostheses depends on harmonious gingival contour and restoration design.[1] Proper emergence profile, papilla preservation, and hygiene are achieved through well-designed healing abutments.[2] While standard abutments do not accurately replicate the natural tooth–gingiva relationship,[3–5] custom abutments better preserve gingival morphology after extraction[6,7] and provide a more favorable emergence profile.[8] Custom abutments also maintain alveolar contour, support gingival health, and reduce plaque accumulation.[9] In grafted sites, they help stabilize the graft without sutures[10,11] while preventing tissue compression[12] and improving esthetics through optimal gingival positioning.[8]

Materials used for custom healing abutments include polymethyl methacrylate (PMMA), polyetheretherketone (PEEK), zirconia, titanium, and resin composite, used alone or in combination.[3] Traditionally fabricated using conventional techniques such as adding flowable resin composite to interim abutments.[13–16] These restorations can now be digitally designed with computer-aided design and computer-aided manufacturing (CAD-CAM) systems and placed at surgery.[11]

The authors declare that they have no known competing financial interests or personal relationships that could have appeared to influence the work reported in this paper.
[a]Dr, Department of Prosthodontics, Faculty of Dentistry, Yeditepe University, Istanbul, Turkey.
[b]Assistant Professor, Department of Prosthodontics, Faculty of Dentistry, Istanbul Galata University, Istanbul, Turkey.
[c]Professor, Department of Prosthodontics, Faculty of Dentistry, Yeditepe University, Istanbul, Turkey.
[d]Professor and Department Head, Department of Prosthodontics, Faculty of Dentistry, Istanbul Galata University, Istanbul, Turkey.

Clinical Implications

The surface characteristics of custom healing abutments may be altered during routine decontamination. Understanding how different treatments interact with 3D printed resins and PEEK may help clinicians select protocols that minimize surface alterations.

Advances in digitally assisted dentistry have also increased the use of 3-dimensionally (3D) printed resins because of their affordability, biocompatibility, polishability, and favorable mechanical properties.[17]

Adequate oral hygiene is critical for implant success but may be compromised in elderly or disabled patients.[18,19] Healing abutments can serve as plaque-retentive surfaces, increasing the risk of complications if not properly maintained.[20] Decontamination methods include mechanical, chemical, and laser-assisted approaches, such as curettes, ultrasonic devices, air-polishing, and agents like chlorhexidine, hydrogen peroxide, and citric acid. Erbium-doped yttrium aluminum garnet (Er:YAG) and diode lasers effectively remove biofilm with minimal surface damage, while electrolytic systems such as GalvoSurge provide additional maintenance options.[17,21–27] Although decontamination methods effectively remove biofilm, they may alter the surface properties of healing abutments because of unavoidable contact, potentially increasing plaque accumulation and affecting peri-implant tissues.[28–32] Therefore, evaluating treatment-induced surface changes is essential.[33] However, current evidence remains limited, and this study aimed to address this gap and contribute to improved long-term prosthetic and periodontal outcomes.

Although previous studies have evaluated laser–material interactions in resin-based materials and PEEK, they have focused mainly on bond strength or isolated laser applications.[34–41] Evidence of their surface effects on contemporary 3D printed dental resins remains limited. In addition, some recently introduced materials such as VarseoSmile TriniQ have not been much investigated, particularly in terms of their response to different decontamination protocols. Furthermore, although electrolytic cleaning systems such as GalvoSurge have been studied for implant decontamination, their effects on additively manufactured polymer-based healing abutments are not well established.[42,43] Therefore, evaluating the combined effects of laser, mechanical, and electrolytic treatments on 3D printed resins and PEEK is clinically relevant.

Accordingly, this study aimed to evaluate and compare the effects of laser modalities, airborne-particle abrasion, and electrolytic cleaning on the surface roughness and morphology of 3D printed resin and the PEEK materials used for custom healing abutments. The null hypothesis was that the applied surface treatment methods would not significantly affect the surface roughness or morphology of the tested materials.

MATERIAL AND METHODS

In this in vitro study, the effects of different surface treatments on the surface roughness and morphology of 3D printed resin and PEEK materials were evaluated. Standardized disk-shaped specimens from three 3D printed resins and one PEEK material were subjected to Er:YAG, neodymium-doped yttrium aluminum garnet (Nd:YAG), diode laser irradiation, airborne-particle abrasion, and electrolytic cleaning (GalvoSurge). Surface roughness was measured before and after treatment using contact profilometry, and representative surface morphology was assessed by scanning electron microscopy.

Three 3D printed resin materials and one PEEK material were used: VarseoSmile TriniQ (BEGO GmbH & Co KG),[44] Saremco Print Crowntec (Saremco Dental AG),[45] C&B Ceramic Resin (Dentafab; 3BFAB Teknoloji AŞ),[46] and CopraPeek (White Peaks Dental Solutions). The sample size was determined by power analysis using surface roughness (Ra) as the primary outcome. An effect size of 0.40 was assumed based on previous studies of surface treatments for polymer-based materials. With α=.05 and a power of.80, the minimum sample size was n=6 per subgroup; this was increased to *n*=12 to improve robustness and reduce variability. Specimens were allocated to 5 treatment groups: Er:YAG laser, Nd:YAG laser, diode laser, airborne-particle abrasion, and GalvoSurge (*n*=48 per group), totaling 240 specimens.

Disk-shaped resin specimens (Ø10×3 mm)[47] were fabricated from standard tessellation language (STL) data using a printer with spark plasma sintering (SPS) technology (ASIGA MAX UV; Asiga) according to the manufacturers' instructions. Postpolymerizing of Saremco Print Crowntec and VarseoSmile TriniQ was performed using 5000 flashes in a nitrogen unit (Otoflash; NK Optik), while Dentafab C&B Ceramic Resin was postpolymerized in a nitrogen unit (Otoflash G-171; NK Optik). PEEK specimens were milled from prefabricated blocks using STL data with a 5-axis CAD-CAM milling unit (CORiTEC 550i; Imes-Icore GmbH, Yamazaki Mazak). Specimens were then sectioned to a height of 3 mm under water cooling using a cutting device (Mecatome T180; Presi). To standardize specimen surfaces, sequential polishing was performed under water cooling using silicon carbide papers (600, 800, 1000, and 1200 grit) (Worth Sanayi Ürünleri Tic Ltd Şti) on a polishing machine (Minitech 233; Presi) at 250 rpm for 30 seconds. Specimen thickness and diameter were then remeasured using digital calipers (Digimatic Caliper 500–196-30; Mutitoyo America Corp). Specimens were subsequently cleaned in an ultrasonic bath with 90% alcohol and immersed in distilled water for 15 minutes.

The laser parameters used in this study were selected based on previously published studies[34,36–40] and to reflect the clinically relevant settings reported for surface treatment and decontamination procedures. These parameters were standardized to allow direct comparison between different laser modalities and to simulate commonly applied clinical protocols. Er:YAG laser irradiation (LightWalker AT; Fotona) was performed at 2940 nm, 150 mJ, 10 Hz, 1.5 W, and 113.04 J/cm² using an H02 handpiece in noncontact mode, perpendicular to the specimen surface at a distance of 10 mm for 20 seconds under water cooling.[34,35] For Nd:YAG laser treatment, specimen surfaces were coated with a carbon-containing marker to enhance absorption.[42] Irradiation (LightWalker AT; Fotona) was performed at 1064 nm using a 300-μm fiber, with 150 mJ, 20 Hz, 3 W, and 2123.1 J/cm², applied perpendicularly at a distance of 10 mm for 20 seconds under water cooling.[34,36] Diode laser irradiation (Woodpecker DTE D-Laser Blue; Woodpecker) was performed at 976 nm using a 300-μm fiber, with 300 mJ, 1.2 W, and 555.5 J/cm², applied perpendicularly at a distance of 10 mm for 20 seconds under water cooling.[34,38] Airborne-particle abrasion was performed using an air-flow device (Air-Flow Handy 2+; EMS) with 50-μm aluminum oxide particles applied at 100% power from a distance of 5 mm for 60 seconds[48] A cleaning system (GalvoSurge Dental Implant Cleaning System; GalvoSurge Dental AG) was applied according to the manufacturer's instructions by securing the device head onto the specimens and delivering an electrolytic current for 2 minutes. The cleaning solution, containing sodium formate, hydroxycarboxylic acid sodium salt, and distilled water, was pumped from the reservoir and evenly distributed over the specimen surfaces. The device automatically stopped at the end of the cycle.[42,43]

After surface treatments, the specimens were ultrasonically cleaned for 60 seconds and dried. Surface roughness (Ra) was measured at baseline (T0) and posttreatment (T1) using a profilometer (Perthometer M1; Mahr GmbH). A 5-μm diamond stylus traversed the surface under a 0.75 mN load at 0.5 mm/second over 350 μm. The device was calibrated before each measurement. For each specimen, measurements were obtained from 3 points in a clockwise direction and averaged to obtain a single value.[34,49] A total of 240 specimens (720 T0 and 720 T1 measurements) were analyzed. All measurements were performed by a single investigator to ensure consistency, consistent with previous studies using a single-operator approach in contact profilometry for surface roughness evaluation.[31,34]

From each group, 1 specimen with a surface roughness value closest to the group mean was selected for scanning electron microscopy (SEM). The specimens were dried at 37 °C for 24 hours and sputter-coated with gold–palladium (EM ACE200; Leica). Surface morphology was examined using a scanning electron microscope (Zeiss EVO LS10 VP; Zeiss), and photomicrographs were obtained at ×1000 magnification.

The data were analyzed using a statistical software package (IBM SPSS Statistics for Windows, v28; IBM Corp). The normality of the data was assessed using the Shapiro–Wilk test, and homogeneity of variance was evaluated using the Levene test. Because of the nonnormal distribution of the data, comparisons between groups were conducted using the Kruskal–Wallis H test, while pairwise intergroup comparisons were performed using the Mann–Whitney *U* test. For each material, specimens were allocated into 5 treatment groups (n=12); every specimen was individually numbered, and posttreatment (T1) measurements were obtained from the same specimens, enabling paired comparisons and minimizing interspecimen variability. To account for baseline differences among materials, treatment effects were primarily evaluated using within-group comparisons between baseline (T0) and posttreatment (T1) measurements. Additionally, the comparison of specimens before and after surface treatments was evaluated using the Wilcoxon signed-rank test (α=.05).

RESULTS

The Shapiro-Wilk test indicated that the data were not normally distributed (P<.05 for all groups); homogeneity of variance was not consistently met according to the Levene test; therefore, nonparametric statistical analyses were performed. The mean surface roughness values for each group are presented in Table 1. Significant intergroup differences were found at baseline (T0), with the lowest value observed for the TriniQ group and the highest value observed for the PEEK group. From T0 to T1, in all groups, the airborne-particle abrasion and Er:YAG treatments were observed to statistically significantly increase surface roughness values compared with baseline values (P<.05). Following the GalvoSurge treatment, no significant difference was observed in the TriniQ and PEEK groups (P>.05), whereas a statistically significant difference was observed in the C&B and Crowntec groups. After Nd:YAG treatment, no significant difference was found in the TriniQ and C&B groups (P>.05), while the roughness values significantly increased in the Crowntec and PEEK groups (P<.05). Following the Diode application, no significant increase was observed in the TriniQ, C&B, or PEEK groups (P>.05), whereas a statistically significant increase was found in the Crowntec group (P<.05).

At T1, the surface roughness values in the TriniQ, C&B, and Crowntec groups were observed to follow the following trend based on pairwise comparisons: Airborne-particle abrasion>Er-YAG>GalvoSurge=Nd-YAG=Diode. In the PEEK group, the surface roughness

Table 1. Mean ±SD roughness values (Ra, μm) of materials evaluated

Surface Treatments							+P
		Airborne-particle abrasion	GalvoSurge	Er-YAG	Nd-YAG	Diode	
Product		Mean ±SD	Mean ±SD	Mean ±SD	Mean ±SD	Mean ±SD	
TriniQ	T0	0.10 ±0.02^{a,A}	0.09 ±0.02^{a,A}	0.09 ±0.02^{a,A}	0.09 ±0.01^{a,A}	0.10 ±0.02^{a,A}	
	T1	0.55 ±0.09^{b,A}	0.09 ±0.02^{a,B}	0.24 ±0.03^{b,C}	0.10 ±0.02^{a,B}	0.11 ±0.05^{a,B}	*
	++p	.002	.295	.002	.456	.248	
C&B	T0	0.10 ±0.02^{a,A}	0.10 ±0.02^{a,A}	0.09 ±0.02^{a,A}	0.09 ±0.01^{a,A}	0.09 ±0.02^{a,A}	
	T1	0.77 ±0.07^{b,A}	0.12 ±0.02^{b,B}	0.17 ±0.04^{b,C}	0.10 ±0.03^{a,B}	0.09 ±0.02^{a,B}	*
	++p	.002	.010	.002	.239	.169	
Crowntec	T0	0.09 ±0.01^{a,A}	0.10 ±0.02^{a,A}	0.10 ±0.01^{a,A}	0.10 ±0.02^{a,A}	0.10 ±0.02^{a,A}	
	T1	0.89 ±0.09^{b,A}	0.12 ±0.02^{b,B}	0.32 ±0.08^{b,C}	0.12 ±0.03^{b,B}	0.13 ±0.04^{b,B}	*
	++p	.002	.028	.002	.045	.002	
PEEK	T0	0.14 ±0.04^{a,A}	0.12 ±0.03^{a,A}	0.11 ±0.02^{a,A}	0.13 ±0.03^{a,A}	0.13 ±0.03^{a,A}	
	T1	0.53 ±0.05^{b,A}	0.12 ±0.03^{a,B}	0.33 ±0.08^{b,C}	0.16 ±0.03^{b,D}	0.14 ±0.05^{a,BD}	*
	++p	.002	.754	.002	.012	.146	

Er-YAG, erbium-doped yttrium aluminum garnet; Nd-YAG, neodymium-doped yttrium aluminum garnet; PEEK, polyetheretherketone; Ra, surface roughness; SD, standard deviation; T0, baseline; T1, posttreatment. Lowercase letters in-group (columns), uppercase letters (rows) indicate statistical difference between groups. *$P<.05$. $^{+}$Kruskal-Wallis test. $^{++}$Wilcoxon signed-rank test.

values were statistically ranked as airborne-particle abrasion>Er-YAG>Nd-YAG ≥Diode=GalvoSurge.

Representative SEM images under ×1000 magnification corroborated the profilometric findings (Figs. 1, 2). The untreated control specimens (Fig. 1) exhibited relatively smooth surfaces. The 3D printed resin materials showed visible layer patterns and minor surface irregularities characteristic of additive manufacturing, whereas PEEK specimens demonstrated a more homogeneous surface with subtle machining marks.

Following surface treatments (Fig. 2), the surface morphology varied depending on the method and material. Airborne-particle abrasion caused pronounced alterations in all materials, with grooves, pits, and disrupted topography. Er:YAG laser also produced noticeable changes, including localized pits and surface irregularities. Nd:YAG effects were material-dependent, with minimal changes in TriniQ and C&B but localized irregularities in Crowntec and PEEK. Diode laser caused minimal alterations overall, except for localized irregularities in Crowntec. GalvoSurge resulted in limited changes, preserving surface features in TriniQ and PEEK while causing mild irregularities in C&B and Crowntec. Overall, SEM findings confirmed treatment- and material-dependent surface changes, consistent with roughness measurements.

DISCUSSION

The null hypothesis that the applied surface treatment methods would not significantly affect the surface roughness or morphology of the tested materials was rejected, as surface treatments significantly affected the surface roughness of 3D printed resin and PEEK materials, with differences depending on both treatment type and material ($P<.05$). The surface treatment protocols evaluated, including laser irradiation, airborne-particle abrasion, and electrolytic cleaning, were selected to represent commonly used clinical decontamination methods for peri-implant maintenance and peri-implantitis therapy. These approaches have been widely applied to remove biofilm and surface contaminants from implant components, including healing abutments.[17,21,28,29,43,48] Among the evaluated materials, Crowntec showed the greatest susceptibility to surface roughening, with significant increases after all treatments, including GalvoSurge, neodymium-doped yttrium aluminum garnet (Nd:YAG), and diode laser ($P<.05$). In contrast, TriniQ and PEEK were more resistant, particularly after GalvoSurge and diode laser ($P>.05$). These differences may be related to variations in resin composition, filler distribution, and polymer structure, affecting surface hardness and laser–material interaction. Materials with higher filler content or

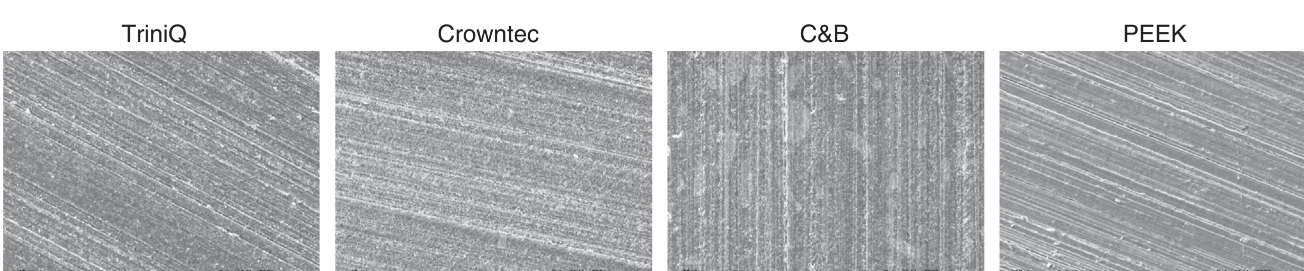

Figure 1. Representative scanning electron microscopy (SEM) images of materials before surface treatments. Original magnification ×1000.

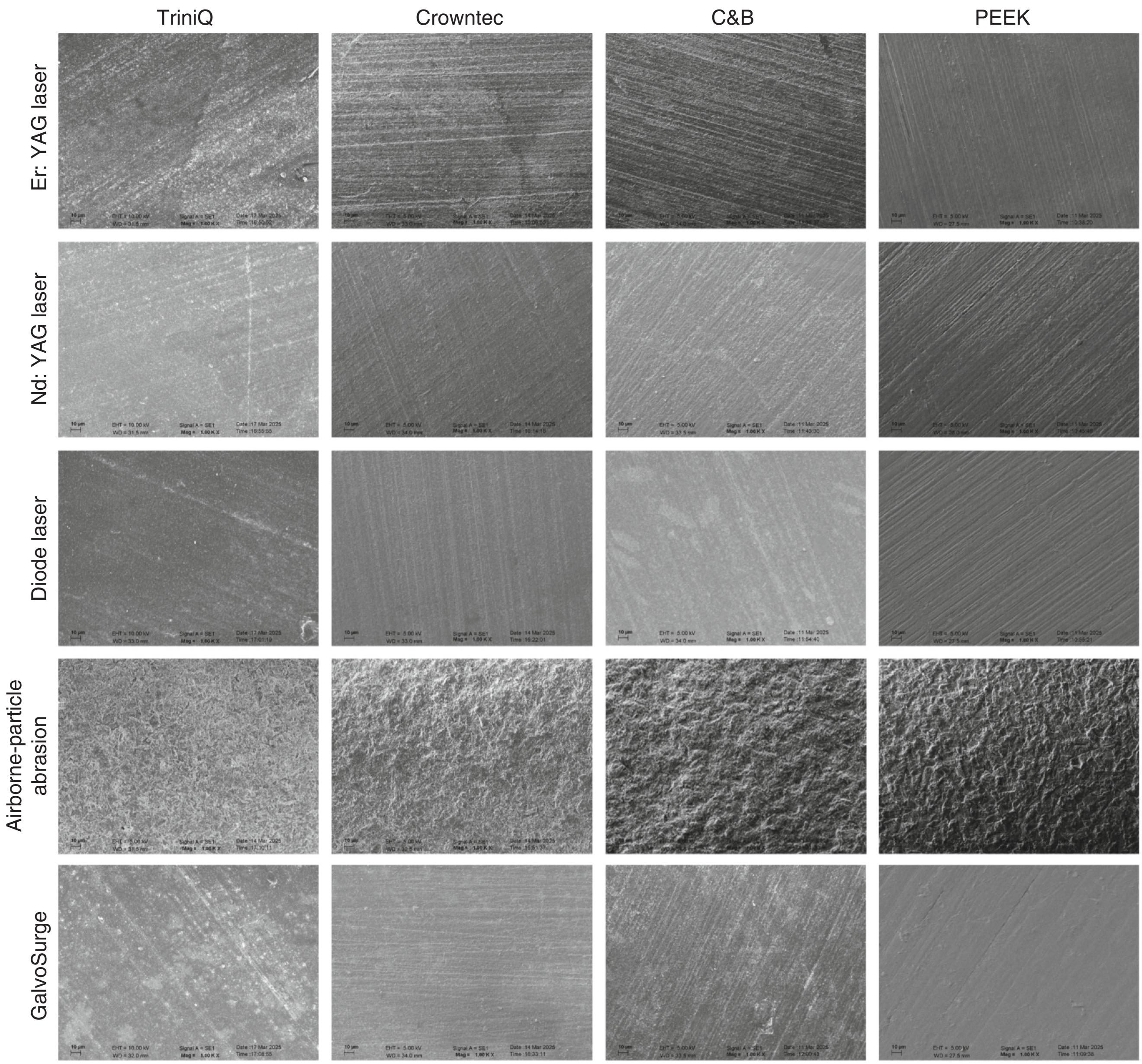

Figure 2. Representative scanning electron microscopy (SEM) image of materials after surface treatments. Original magnification ×1000.

ceramic reinforcement may exhibit greater surface disruption because of differential ablation of organic and inorganic phases.[30,31] The stability of PEEK is likely related to its semicrystalline structure and high thermal stability, which limit surface damage under non-aggressive treatments.[34,35,42]

Airborne-particle abrasion and Er:YAG laser produced the greatest increases in surface roughness, with significant changes in all groups ($P<.05$). Airborne-particle abrasion yielded the highest Ra values, particularly in Crowntec, reflecting aggressive mechanical roughening because of high-velocity particle impact, consistent with previous studies.[22,23] Similarly, Er:YAG laser significantly increased roughness in all materials, likely because of thermomechanical ablation, where rapid water-mediated heating causes micro-explosions, resulting in pits and surface irregularities.[24,38,39] In contrast, Nd:YAG and diode lasers showed material-dependent effects, with significant increases mainly in Crowntec and, for Nd:YAG, PEEK ($P<.05$), while TriniQ and C&B remained largely unaffected ($P>.05$). The higher susceptibility of Crowntec may be related to its heterogeneous filler–matrix structure, increasing sensitivity to thermal stress.[39,45] The roughening of PEEK after Nd:YAG may be attributed to photothermal effects at 1064 nm, causing localized melting and resolidification, further influenced by its semicrystalline structure.[34,39,41] In contrast, the more homogeneous methacrylate-based structure of TriniQ and C&B may explain their lower surface alteration.[39,44,46]

GalvoSurge treatment showed a conservative effect on surface roughness, with no significant changes in TriniQ and PEEK (P>.05) and with mild increases in C&B and Crowntec (P<.05), remaining lower than airborne-particle abrasion and Er:YAG. This supports its electrolytic mechanism, which removes biofilm without mechanical or thermal damage. Previous studies report similarly effective decontamination with preserved surface topography.[43,48] The limited surface alteration was likely because of the mild chemical composition of the cleaning solution, primarily containing sodium formate and weak organic acid salts, which disrupt biofilm without degrading the polymer matrices or filler phases. Consequently, the absence of strong oxidizing or acidic components likely minimizes matrix softening and filler–matrix interface damage.[25,26,43]

Clinically, these findings are relevant, as excessive surface roughening has been associated with increased plaque accumulation and peri-implant inflammation.[32] A roughness threshold of approximately 0.2 µm (Ra) has been proposed as critical for bacterial retention.[32] Therefore, treatments that achieve decontamination while preserving surface integrity may be preferable for the long-term use of custom healing abutments.[32] However, surface roughness remains an indirect indicator, as biofilm formation and tissue response are also influenced by material properties and host-related factors.

The pronounced roughening effect of airborne-particle abrasion on 3D printed resins is consistent with Kang et al,[27] who reported significant roughness increases following the alumina airborne-particle abrasion of UDMA- and BEMA-based resins, associated with porous morphology and surface irregularities caused by high-velocity particle impact. Similar findings were observed in the present study, particularly in Crowntec and TriniQ (P<.05). Regarding laser effects on PEEK, the results partially agree with those of Asik et al,[34] who reported increased roughness with all laser types. Although laser application increased Ra values in this study, Er:YAG produced significantly greater roughness than Nd:YAG and diode lasers (P<.05), likely because of differences in laser parameters, energy density, and cooling conditions.

Although laser–material interactions have been studied in resin-based materials and PEEK,[34–39] existing research has primarily focused on surface wettability, ablation behavior, and bond strength in conventional materials, with limited data on contemporary 3D printed dental resins and their response to laser-based decontamination. Evidence on newer materials such as VarseoSmile TriniQ has been particularly scarce, especially regarding their response to different decontamination methods. Similarly, while electrolytic systems like GalvoSurge are used for implant decontamination, their effects on additively manufactured polymer-based healing abutments remain unclear.[42,43] Therefore, direct comparisons with the literature are limited, and the present findings may provide a preliminary basis for future research in this field.

Limitations of this study included the in vitro design that cannot fully replicate the dynamic oral environment, including salivary flow, temperature variations, and biofilm maturation. In addition, only a single parameter set was used for each surface treatment; different laser settings or exposure times may yield different results. Moreover, biological outcomes such as biofilm formation and cellular responses were not evaluated; therefore, the clinical implications of the observed surface roughness changes should be interpreted with caution. Flat disk-shaped specimens were used to standardize measurements, but this approach does not fully represent the complex geometry of clinical healing abutments. Future studies should use in vitro biofilm models or in vivo designs to better reflect clinical conditions, investigate a broader range of laser parameters and exposure times, and incorporate biological endpoints such as cell viability and bacterial adhesion assays.

CONCLUSIONS

Based on the findings of this in vitro study, the following conclusions were drawn:

1. Surface treatments affected the roughness and morphology of 3D printed resin and PEEK materials in a material- and method-dependent manner.
2. Airborne-particle abrasion and Er:YAG produced the greatest roughness increases within each material, whereas diode laser and GalvoSurge largely preserved surface integrity.
3. Neodymium-doped yttrium aluminum garnet (Nd:YAG) showed material-dependent effects, with notable increases in Crowntec and PEEK.
4. These findings suggested that surface treatment selection for custom healing abutments should be material-specific, as excessive roughening may be associated with increased plaque accumulation.

REFERENCES

1. Forna N, Agop-Forna D. Esthetic aspects in implant-prosthetic rehabilitation. *Med Pharm Rep*. 2019;92:6–13.
2. Hung CCU, Costa RC, Pereira G, Abdo VL, Noronha MS, Retamal-Valdes B, et al. Oral microbial colonization on titanium and polyetheretherketone dental implant healing abutments: An in vitro and in vivo study. *J Prosthet Dent*. 2025;133:1545–1552.
3. Chokaree P, Poovarodom P, Chaijareenont P, Yavirach A, Rungsiyakull P. Biomaterials and clinical applications of customized healing abutment: A narrative review. *J Funct Biomater*. 2022;13:291.
4. Lemongello GJ. Customized provisional abutment and provisional restoration for an immediately placed implant. *Pract Proced Aesthet Dent*. 2007;19:419–424.

5. Wittneben JG, Buser D, Belser UC, Brägger U. Peri-implant soft tissue conditioning with provisional restorations in the esthetic zone: The dynamic compression technique. *Int J Periodontics Restorative Dent*. 2013;33:447–455.
6. Resnik RR, Misch CE. Misch's Contemporary Implant Dentistry. 4th ed.. Elsevier; 2021.
7. Weigl P, Trimpou G, Grizas E, Hess P, Nentwig GH, Lauer HC, et al. All-ceramic versus titanium-based implant-supported restorations: Preliminary 12-month results from a randomized controlled trial. *J Adv Prosthodont*. 2019;11:48.
8. Lertwongpaisan T, Amornsettachai P, Panyayong W, Suphangul S. Soft tissue dimensional change using customized titanium healing abutment in immediate implant placement in posterior teeth. *BMC Oral Health*. 2023;23:384.
9. Ruales-Carrera E, Pauletto P, Apaza-Bedoya K, Volpato CAM, Ozcan M, Benfatti CAM. Peri-implant tissue management after immediate implant placement using a customized healing abutment. *J Esthet Restor Dent*. 2019;31:533–541.
10. Hu C, Gong T, Lin W, Yuan Q, Man Y. Immediate implant placement into posterior sockets with or without buccal bone dehiscence defects: A retrospective cohort study. *J Dent*. 2017;65:95–100.
11. Chokaree P, Poovarodom P, Chaijareenont P, Rungsiyakull P. Effect of customized and prefabricated healing abutments on peri-implant soft tissue and bone in immediate implant sites: A randomized controlled trial. *J Clin Med*. 2024;13:886.
12. Ruhstorfer M, Güth JF, Stimmelmayr M, Waltenberger L, Schubert O, Graf T. Systematic review of peri-implant conditions and esthetic outcomes of customized versus conventional healing abutments. *Int J Implant Dent*. 2024;10:61.
13. Chu SJ, Hochman MN, Tan-Chu JHP, Mieleszko AJ, Tarnow DP. A novel prosthetic device and method for guided tissue preservation of immediate postextraction socket implants. *Int J Periodontics Restor Dent*. 2014;34:S9–S17.
14. Akin R. A new concept in maintaining the emergence profile in immediate posterior implant placement: The anatomic harmony abutment. *J Oral Maxillofac Surg*. 2016;74:2385–2392.
15. Pow EHN, McMillan AS. A modified implant healing abutment to optimize soft tissue contours: A case report. *Implant Dent*. 2004;13:297–300.
16. Stumpel LJ, Wadhwani C. Development and capture of soft tissue contours at time of implant placement. *J Prosthet Dent*. 2017;117:709–713.
17. Dhaliwal JS, Abd Rahman NA, Ming LC, Dhaliwal SKS, Knights J, Albuquerque Junior RF, et al. Microbial biofilm decontamination on dental implant surfaces: A mini review. *Front Cell Infect Microbiol*. 2021;11:736186.
18. Girestam Croonquist C, Dalum J, Skott P, Sjögren P, Wårdh I, Morén E. Effects of domiciliary professional oral care for care-dependent elderly in nursing homes: Oral hygiene, gingival bleeding, root caries and nursing staff's oral health knowledge and attitudes. *Clin Interv Aging*. 2020;15:1305–1315.
19. Lauritano D, Moreo G, Della Vella F, Di Stasio D, Carinci F, Lucchese A, et al. Oral health status and need for oral care in an aging population: A systematic review. *Int J Environ Res Public Health*. 2019;16:4558.
20. De Visschere LM, Grooten L, Theuniers G, Vanobbergen JN. Oral hygiene of elderly people in long-term care institutions: A cross-sectional study. *Gerodontology*. 2006;23:195–204.
21. Jordan A, Smojver I, Budimir A, Gabrić D, Vuletić M. Evaluation of different procedures for titanium dental implant surface decontamination: An in vitro study. *Bioengineering (Basel)*. 2024;11:326.
22. Stawarczyk B, Taufall S, Roos M, Schmidlin PR, Lümkemann N. Bonding of composite resins to polyetheretherketone: The influence of adhesive systems and air-abrasion parameters. *Clin Oral Investig*. 2018;22:763–771.
23. Güler AU, Duran I, Yücel AÇ, Özkan P. Effects of air polishing powders on the surface roughness of composite resins. *J Dent Sci*. 2010;5:136–143.
24. Melo-Soares V, Gazott-Simões I, Dos Reis AC, Valente MLC. Effect of surface pretreatment with erbium-doped yttrium aluminum garnet laser on hydroxyapatite coating adhesion and mechanical properties of titanium alloy discs. *Lasers Med Sci*. 2025;40:130.
25. Ratka C, Weigl P, Henrich D, Koch F, Schlee M, Zipprich H. The effect of in vitro electrolytic cleaning on biofilm-contaminated implant surfaces. *J Clin Med*. 2019;8:1397.
26. Klein A, Rasperini G, Gruber R, Andrukhov O, Rausch-Fan X. Electrolytic cleaning of dental implants: A scoping review of clinical studies. *Dent J (Basel)*. 2025;13:172.
27. Kang YJ, Kim H, Lee J, Park Y, Kim JH. Effect of airborne particle abrasion treatment of two types of three-dimensional printing resin materials for permanent restoration materials on flexural strength. *Dent Mater*. 2023;39:648–658.
28. Schwarz F, Sahm N, Iglhaut G, Becker J. Impact of the method of surface debridement and decontamination on the clinical outcome following combined surgical therapy of peri-implantitis: A randomized controlled clinical study. *J Clin Periodontol*. 2011;38:276–284.
29. John G, Becker J, Schwarz F. Rotating titanium brush for plaque removal from rough titanium surfaces: An in vitro study. *Clin Oral Implants Res*. 2014;25:838–842.
30. Kara D, Tekçe N, Fidan S, Demirci M, Tuncer S, Balcı S. The effects of various polishing procedures on surface topography of CAD/CAM resin restoratives. *J Prosthodont*. 2021;30:481–489.
31. Alhassan M, Maawadh A, Labban N, Alnafaiy SM, Alotaibi HN, BinMahfooz AM, et al. Effect of different surface treatments on the surface roughness and gloss of resin-modified CAD/CAM ceramics. *Appl Sci (Basel)*. 2022;12:11972.
32. Bollen CM, Lambrechts P, Quirynen M. Comparison of surface roughness of oral hard materials to the threshold surface roughness for bacterial plaque retention: A review of the literature. *Dent Mater*. 1997;13:258–269.
33. Sousa V, Mardas N, Spratt D, Hassan IA, Walters NJ, Beltrán V, et al. The effect of microcosm biofilm decontamination on surface topography, chemistry, and biocompatibility dynamics of implant titanium surfaces. *Int J Mol Sci*. 2022;23:10033.
34. Asik B, Ozyilmaz OY. Effects of various laser applications on surface roughness and bond strength to veneering composites of polyether ether ketone and polyether ketone ketone materials. *Lasers Med Sci*. 2024;39:269.
35. Caglar I, Ates SM, Yesil Duymus Z. An in vitro evaluation of the effect of various adhesives and surface treatments on bond strength of resin cement to polyetheretherketone. *J Prosthodont*. 2019;28:e342–e349.
36. Ulgey M, Gorler O, Karahan Gunduz C. Effects of laser modalities on shear bond strengths of composite superstructure to zirconia and polyetheretherketone infrastructures: An in vitro study. *Odontology*. 2021;109:845–853.
37. Lawrence J, Li L. Modification of the wettability characteristics of polymethyl methacrylate by means of CO2, neodymium-doped yttrium aluminum garnet, excimer, and high-power diode laser radiation. *Mater Sci Eng A*. 2001;303:142–149.
38. Kim ME, Jeoung DJ, Kim KS. Effects of water flow on dental hard tissue ablation using erbium-doped yttrium aluminum garnet laser. *J Clin Laser Med Surg*. 2003;21:139–144.
39. Tzanakakis EGC, Skoulas E, Pepelassi E, Koidis P, Tzoutzas IG. The use of lasers in dental materials: A review. *Materials (Basel)*. 2021;14:3370.
40. Angelova L, Filipov E, Avdeev G, Daskalova A. Surface modification of polyetheretherketone via femtosecond laser microprocessing for enhanced bioactivity: A preliminary study. *Bioengineering (Basel)*. 2025;12:1285.
41. Riveiro A, Soto R, Comesaña R, Boutinguiza M, del Val J, Quintero F, et al. Laser surface modification of polyetheretherketone. *Appl Surf Sci*. 2012;258:9437–9442.
42. Schlee M, Rathe F, Brodbeck U, Ratka C, Weigl P, Zipprich H. Treatment of peri-implantitis: Electrolytic cleaning versus mechanical and electrolytic cleaning: A randomized controlled clinical trial: Six-month results. *J Clin Med*. 2019;8:1909.
43. Assunção MA, Botelho J, Machado V, Proença L, Matos APA, Mendes JJ, et al. Dental implant surface decontamination and surface change of an electrolytic method versus mechanical approaches: A pilot in vitro study. *J Clin Med*. 2023;12:1703.
44. BEGO Bremer Goldschlägerei Wilh Herbst GmbH & Co. KG. VarseoSmile TriniQ. 2026.
45. SAREMCO Dental AG. Instruction for use: Saremco Print Crowntec. 2023.
46. 3BFAB Teknoloji AŞ. Power resins Dentafab. 2023.
47. Bezerra PTM, deSousa LC, Pereira ALC, Bezerra ALCA, deSouza Borges Grisi MH, deFátima Dantas de Almeida L, et al. In vitro effect of simulated brushing on color stability, surface roughness, and microbial adhesion of characterizing resin composites for 3D-printed denture bases. *J Prosthodont* 2025:1–9.
48. Leung K, Bi J, Giannelis G, Owen G, Larjava H. Decontamination of multispecies oral biofilm from rough implant surface by airflow with glycine. *Clin Exp Dent Res*. 2022;8:322–328.
49. Solanki A, Manan R, Dayal C, Mohan M, Gupta A, Ashiq N, Gupta S. Assessment of surface roughness of composite resins polished with different systems and speeds: A comparative in vitro study. *Cureus*. 2025;17:11.

Corresponding author:
Prof Ozgun Yusuf Ozyilmaz
Department of Prosthodontics
Istanbul Galata University
Haciahmet, Irmak Caddesi DLP 1-9 Beyoglu
Istanbul 34440
TURKEY

Email: ozgunyusufozyilmaz@gmail.com

https://doi.org/10.1016/j.prosdent.2026.07.029